Composites Part B 165 (2019) 365–378

Contents lists available at ScienceDirect

Composites Part B

journal homepage: www.elsevier.com/locate/compositesb

Effect of surface treatment on quasi-static compression and dynamic mechanical analysis of syntactic foams

Mrityunjay Doddamani

Department of Mechanical Engineering, National Institute of Technology Karnataka, Surathkal, 575025, India

ARTICLE INFO

Keywords:
Surface modification
Cenospheres
Quasi-static compression
Dynamic mechanical analysis
Syntactic foams

ABSTRACT

Quasi static compression (10^{-1}, 10^{-2} and 10^{-3} s^{-1} strain rates) and dynamic mechanical analysis (temperature sweep of 30–175 °C) of cenosphere/epoxy syntactic foams are investigated. Effect of cenosphere content (20, 40 and 60 vol %) and surface modification are presented. Quasi-static tests reveal lower modulus for neat epoxy samples as compared to all the syntactic foams. With increasing cenosphere content and strain rate, elastic modulus increases for all the tested conditions. Foams reinforced with surface modified cenosphere exhibit higher modulus as compared with untreated ones and neat epoxy. Energy absorption of samples increases with increasing cenosphere content and surface modification. Storage modulus of untreated and treated syntactic foams register higher values with increase in cenosphere content and are higher than the neat epoxy samples. Loss modulus of syntactic foams at room temperature are lower as compared with pure epoxy while damping of untreated and treated foams registered higher values as compared with neat resin. Scanning electron microscopy of the samples are performed for structure property correlations. Finally, property map for quasi-static compression is presented by comparing results of present work with the extracted values from literature.

1. Introduction

Syntactic foam is realized by embedding hollow particles in matrix. Ability of these foams to allow flexibility in tailoring desired properties is very attractive and noteworthy [1]. Porosity in these foams is bound within microballoons and hence known as closed cell foams. These foams offer low density and moisture absorption coupled with superior mechanical properties [2]. Such foams are widely used for fabrication of submarine components demanding buoyancy [3,4]. In particular these materials are utilized in marine and aerospace sectors because of their lightweightness and favorable properties [5]. Core materials in sandwich composites are often made by syntactic foams as they provide enhanced stiffness and compressive strength desired by sandwich structures [6]. Hollow microspheres play a vital role in defining syntactic foams behavior Microballoons made up of glass, carbon, fly ash cenospheres, ceramics and expandable polymers perlite spheres are used in the fabrication of syntactic foams [7–12].

Low processing cost of particulate fillers coupled with enhanced mechanical properties, higher dimensional stability and wear resistance makes particulate fillers a viable option to be used in composite materials [13–22]. One such economical and environmentally contaminant filler is fly ash. Thermal power plants are the source for fly ash, generated in abundance and are a waste by-product demanding effective disposal [23,24]. The major constituent in fly ash is cenosphere which are characterized as hollow microballoons [25,26]. SiO_2, Al_2O_3 and Fe_2O_3 are the major constituents of these cenospheres accounting for nearly 90% of its composition [27]. The other compounds such as K_2O, MgO, CaO, TiO_2 and Na_2O are also present but in trace quantities. Low density fly ash cenospheres are very beneficial to attain higher strength to weight ratio [28]. These cenospheres are spherical in shape, available in powder form, inexpensive and possess superior mechanical properties as compared to engineered counterparts [29–34]. Use of industrial waste materials like fly ash cenospheres is gaining more importance in structural applications in order to develop new recycling avenues. These cenosphere particles have built-in porosity within their walls making them more porous. Such unique features cannot be seen in commercially available hollow particles. Moreover, landfill burden and disposal related issues pertaining to fly ash cenospheres can be effectively addressed if these hollow particles are incorporated in most commonly used thermosetting epoxy resin leading to development of utilitarian syntactic foams for specific applications [35,36]. Such developed foams need mechanical characterization particularly in compressive and energy absorption related regimes for proposing suitable applications.

Quasi-static compressive response of these closed cell foams are extensively dealt with in the available literature [37–40] owing to their

E-mail address: mrdoddamani@nitk.edu.in.

https://doi.org/10.1016/j.compositesb.2019.01.076
Received 22 August 2018; Received in revised form 12 January 2019; Accepted 19 January 2019
Available online 25 January 2019
1359-8368/

Nomenclature

ρ	Density of the composite kg/m^3	ρ^{exp}	Density -Experimental kg/m^3
V	Volume fraction %	T_g	Glass transition temperature ˚C
ϕ_V	Void content %	T_{max}	Maximum use temperature ˚C
ρ^{th}	Density - Theoretical kg/m^3	$Tan\ \delta$	Damping factor ——
		E'	Storage modulus MPa
		E''	Loss modulus MPa

high compressive strength, high energy absorption during deformation and high damage tolerance. Swetha and Ravikumar [38] examined epoxy syntactic foams reinforced with hollow glass microspheres and revealed that with increase in wall thickness of hollow particles, reduction in compression strength and elastic modulus is observed. Ahmadi et al. [39] reported decrease in compressive strength, elastic modulus, failure strain and plateau stress with increase in ceramic microballoon volume fraction. Specific strength and modulus increases for 20 and 40 vol.% of filler but decreases with 60 vol % as observed by them. Earlier efforts have focussed on syntactic foams behavior with hollow glass microballoons as fillers [38,39] but studies based on surface modified fly cenospheres are very scarce [37]. Zeltmann et al. [41] revealed cenospheres addition in thermoplastics improve the storage and loss modulus for all the temperatures studied. Threshold storage modulus is improved by about 5 ˚C for syntactic foams as compared to the matrix, indicating better thermal stability. Damping increases with increasing temperature and such increase is most drastic as the melting temperature is approached. Shunmugasamy et al. [42] revealed that at sub-zero and room temperature, increase in microballoon wall thickness at similar volume fraction results in storage modulus rise. Addition of microballoons leads to 14–66% decrease in damping as compared to neat resin and exhibits higher storage modulus post T_g. Das and Satapathy [43] revealed that improvement in the dissipation energy and storage modulus is observed up to 30 wt.% of cenosphere. At lower/sub-zero temperatures (−25 to 0 ˚C), storage modulus increase with cenosphere content. However, elevated temperatures do not show such an improvement.

Tagliavia et al. [44] showed that microsphere particles with higher wall thickness exhibit enhanced storage modulus while it is not monotonically related to microspheres volume fraction. Lin et al. [45] showed that thermal stability increases by increasing microballoon wall thickness while it is relatively less sensitive to microballoon volume fraction. Presence of ceramic content in the microstructure of syntactic foam lowers the coefficient of thermal expansion as compared to the neat matrix. Microballoon content in the composite has a prominent effect on the T_g while the effect of microballoon wall thickness is less significant. Gu et al. [46] revealed that damping capacity is enhanced by fly ash addition which is attributed to increase in frictional damping and hollow structure of fly ash particles. Influence of matrix viscoelasticity is higher whereas frictional energy dissipation is comparatively lesser for cenosphere volume fraction lower than 30%. Between 30 and 50 vol.% of cenosphere, frictional energy dissipation impact is similar to the matrix viscoelasticity. At 70 vol.% of cenosphere, the influence of matrix viscoelasticity drops sharply owing to the severe dilution effect of fly ash cenosphere into the matrix. Sankaran et al. [47] showed that storage modulus present decreasing trend with rise in temperature of the foam as well as neat resin. Syntactic foams present higher T_g as compared to neat resin due to polymeric chains constrained mobility in the matrix/filler interphase.

As received cenospheres possess several defects resulting in inferior properties of the composites. Although the alumino silicate composition compensates for the properties, overall performance of the composites gets hindered due to inferior interfacial bonding. Mussel-inspired chemistry has emerged as a very important surface modification method owing to its gentle experiment conditions, high modification efficiency and universality [48–57]. However, coupling agents such as silane are usually employed to promote adhesion between organic matrix and inorganic filler. Ability of silane coupling agents in promoting adhesion develops a molecular bridge between cenosphere filler and epoxy matrix resulting in covalent bonds that contribute towards enhanced interfacial characteristics between the constituents. Previous studies indicate that hollow microsphere/matrix adhesion plays a significant role in determining the syntactic foam response. Nevertheless, a comprehensive study of these foams with influence of microballoon/matrix bonding on the quasi static compressive and Dynamic Mechanical Analysis (DMA) is lacking.

Current work is aimed at addressing the above mentioned concerns in entirety and to represent the energy absorption capacity. Moreover, no examination of the quasi-static compression behavior of cenosphere reinforced epoxy foams is reported yet. In the present study, epoxy (Lapox L-12) is selected as the matrix material due to its low shrinkage, higher strength and excellent adhesion to various substrates, low cost and low toxicity. These resins are well suited for composite applications as they have greater tendency to wet surfaces of reinforcements. Although, polymeric matrix material for the foams can be selected from a wide variety of thermosetting resins such as cyanate ester [19], polysialate [20] and vinyl ester [21]. Epoxy resins are the most commonly used matrix resin owing to their extensive use in aerospace and marine applications [22]. Further, quasi static compressive and dynamic mechanical tests are performed on cenosphere/epoxy syntactic foam samples. Cenospheres are utilized in both as-received and silane modified forms. Mechanical properties are evaluated as a function of filler content at different strain rates and elevated temperatures. Micrography is performed to analyze structure-property correlations. Finally, property map for quasi-static compression tests is presented that may act as a guideline for choosing appropriate material system depending on the application.

2. Material and methods

2.1. Materials

Epoxy resin (LAPOX L-12) with K6 hardener is used as the matrix material that is supplied from Atul Ltd., Gujarat, India. Cenospheres used as filler for the fabrication of foam specimens and are obtained from Cenosphere India Private Limited, Kolkata, India. Cenospheres physical and chemical analysis details are available in Ref. [32]. Cenospheres are treated using APTS (3-amino propyl triethoxy silane) procured from Sigma Aldrich, Bangalore, India. Surface treatment of cenospheres, fourier transformed infrared spectroscopy for confirming silane treatement on cenospheres, particle size analysis and X-ray diffractograms of cenospheres are presented in Ref's [32,58].

2.2. Syntactic foam fabrication

Foams are prepared with 20, 40 and 60 vol fraction of cenospheres. Fabrication of syntactic foams is carried out in a two-step process of mixing and casting. Initially an intended amount of epoxy is taken into a beaker followed by the addition of required volume fraction of cenospheres. Mixture is gently stirred to achieve a uniform homogeneous slurry. Further, hardener is added by 10 wt.% in the prepared slurry and degassed for 5 min prior to pouring into the aluminium mold. Wax applied on the mold prior to pouring of slurry enables easy removal of cast slabs. Room temperature curing for 24 h with post

curing of 3 h at 90 °C is adopted. Same processing methodology is followed for preparing foams with untreated and silane treated cenospheres. Neat epoxy samples are also fabricated under similar processing environment for comparative analysis. All the specimens are coded as per 'EXXY', where E represents epoxy matrix, XX denotes cenosphere volume percentage and Y represents the filler condition (U and T for untreated and treated respectively). Diamond saw cutter is used to trim the cast slabs according to the required dimensions. Density measurement is carried out as per the method defined in ASTM D792-13 and the average values are considered. Details about densities (theoretical and experimental), void volume fraction and weight saving potential of the developed foams are available in Ref. [32].

2.3. Quasi static testing

Universal testing instrument (Zwick Roell, USA) with 20 kN load cell is utilized to perform quasi-static compression tests. These tests are performed at strain rates of 10^{-3}, 10^{-2} and 10^{-1} s^{-1} corresponding to a cross-head displacement velocity of 0.001, 0.01 and 0.1 mm/min respectively. The condition for end of the test is fixed at 20 kN load. An in-house developed MATLAB code is used for analysing the experimental data. Compressive modulus and strength are calculated for all the specimens. Minimum of five samples in each volume fraction are tested.

2.4. Dynamic mechanical analysis

Dynamic mechanical tests are performed by Q800 DMA, New Castle, DE. Samples with dimensions of 7 × 4 × 50 mm are examined in the dual cantilever arrangement having a span length of 35 mm. Tests are conducted to study the behavior of syntactic foams at elevated temperature using temperature sweep mode (28–175 °C at a constant rate of 1 °C/min with the deformation occurring at a constant frequency of 1 Hz). Testing is stopped once the storage modulus touches a value of 20 MPa to avoid complete melting of the sample. Five specimens of each configuration are tested for DMA.

2.5. Scanning electron microscopy

Scanning electron microscopy (JSM 6380LA, JEOL, Japan) is utilized for microscopic investigation of the tested samples. For better conductivity, all the samples are gold coated (JFC-1600 auto fine coater, JEOL, Japan).

3. Results and discussions

3.1. Materials processing

Fly ash cenospheres are used in both untreated and surface modified conditions to develop syntactic foams. Fig. 1 shows micrographs of untreated and treated fly ash cenospheres at the same magnification levels. Coated silane layer is not clearly recognizable as observed from Fig. 1b owing to its small layer thickness. However, the surface of treated cenospheres (Fig. 1b) appears to be better compared to the untreated one (Fig. 1a). Particle size analysis and FTIR of as received and surface treated cenospheres confirm silane coating [58,59]. These treated cenospheres are expected to improve the interfacial bonding between the constituents. Manual stirring method is used to disperse cenospheres in epoxy resin. Uniform dispersion with minimum particle failure of cenospheres in the matrix is a challenging task. However, micrographs of as cast E60U and E60T foams (Fig. 2a and Fig. 2b) show uniform dispersal of cenospheres within the epoxy matrix, justifying manual stirring method for casting the syntactic foams. E60U foams show poor interfacial bonding (Fig. 2c) while E60T foams exhibit better bonding between the constituents (Fig. 2d). Lower values of experimental density as compared to theoretical results signify intact particles during processing. Incorporation of hollow fly ash cenospheres reduces experimental density of neat epoxy samples by 13.73 and 11.44% respectively in E60U and E60T foams [32].

3.2. Quasi-static compression

3.2.1. Stress-strain response

Stress-strain profiles of quasi-static compression samples tested at varying strain rates are graphed in Fig. 3. Stress-strain response exhibited by all the samples are similar until peak stress. At the end of linear elastic region, drop in stress is observed followed by a stress plateau that resembles distinctive characteristic of foams [38,60]. Since epoxy is brittle in nature, stress drops post linear elastic regime tailed by plateau [61–63]. This drop in stress is attributed to the consecutive brittle failure of cenospheres in epoxy and stress concentration therein [64]. Stress plateau observed in cenosphere/epoxy syntactic foams is not witnessed for thermoplastic syntactic foams [37]. Peak stress values are seen to be decreasing drastically with decreasing strain rates for EXXU foams as compared to EXXT foams. Peak stress values of E20T foam are comparable to neat epoxy response. Further, EXXT foams are seen to be performed better as compared to EXXU foams (Fig. 3) implying influence of surface modification on quasi-static compressive response.

Fig. 4 presents a schematic representation of stress strain curves for the samples in quasi-static compressive mode. Plot is divided into linear elastic, plateau and densification region. In the elastic regime, the specimen is subjected to a uniform deformation resulting in a linear elastic region. The stress attains a maximum value and consequently reaches a constant value as the load increases resulting in the plateau region. Peak stress indicates crack instigation in the matrix (Fig. 3). Once the crack formation takes place, sustained deformation at constant stress is observed conforming to the compressed samples energy absorption. Energy absorption is accredited to the fragmentation of

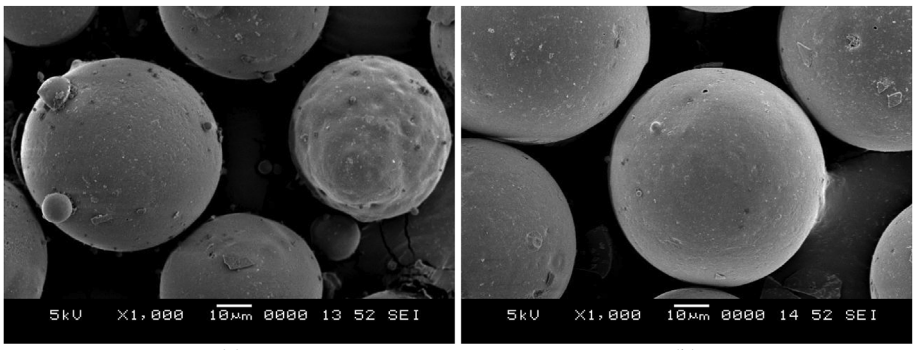

(a) (b)

Fig. 1. (a) As received and (b) treated fly ash cenospheres.

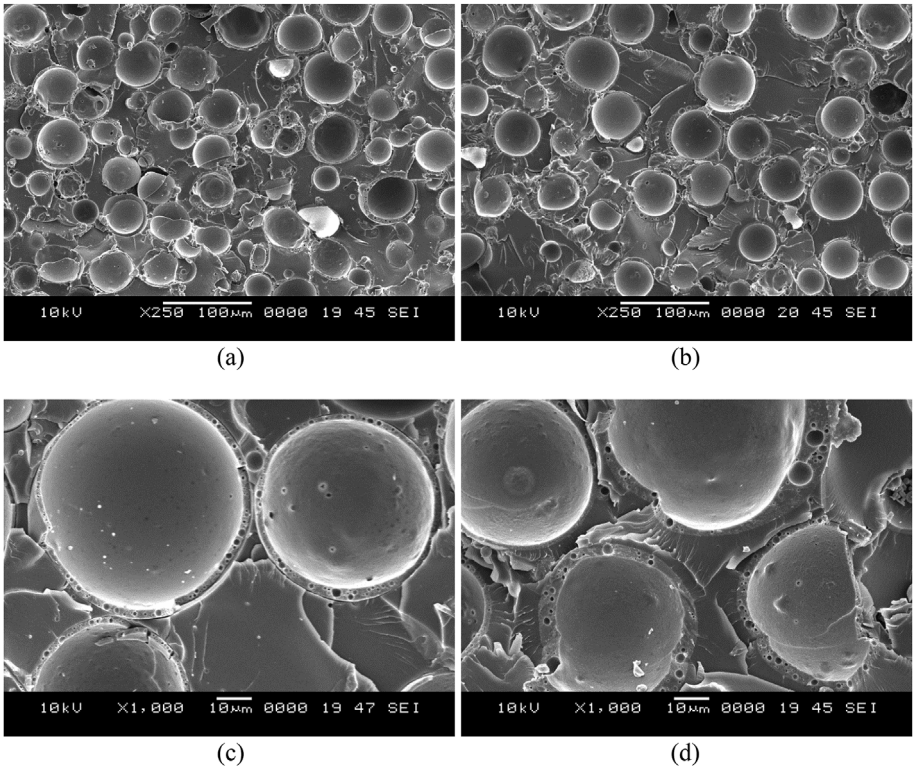

Fig. 2. Micrographs of (a) E60U and (b) E60T. Inferior bonding for E60U can be observed in (c) while silane treatment exhibits good interfacial bonding in (d) E60T.

cenospheres that expose the hollow space from within cenospheres to accommodate the compressed material [60]. Once substantial amount of cenospheres are crushed in compression, stress level starts to increase again representing densification region.

3.2.2. Compressive modulus and strength in quasi-static mode

Mechanical properties of syntactic foams in quasi-static compression are presented in Table 1. Neat epoxy samples register lower modulus as compared to both untreated and treated foams. The average elastic modulus is observed to rise with higher filler content and strain rate for foams (Fig. 5a). Among all the foams, E60T exhibits higher modulus at all the strain rates tested. However, poor interfacial bonding between the constituent compromise modulus values of EXXU. Silane treated syntactic foams registered higher modulus. Compared to the modulus of neat resin at 10^{-1}, 10^{-2} and 10^{-3} s^{-1} strain rates, the modulus increased for EXXU foams in the range of 0.9–27, 15–37, 29–106% while for EXXT foams, modulus increased in the range of 25–79, 28–107, 76–203%, respectively with higher filler loading. All the syntactic foams present higher specific modulus values as compared to E0 (Fig. 5b). E60T at 10^{-1} s^{-1} strain rate registered highest specific modulus as compared to all other compositions making the EXXT foams very suitable for applications demanding lightweight structures with enhanced compressive modulus.

Neat epoxy samples registered higher strength values as compared to all the foams (Fig. 5c). Strength of neat epoxy sample for 10^{-3}, 10^{-2} and 10^{-1} s^{-1} strain rates is 104.62, 116.93 and 126.04 MPa respectively. With increasing filler loading, strength of EXXU and EXXT foams decreases to the tune of 18–26 and 6–9% respectively as against neat epoxy for different strain rates. Increase in the hollow particles content in the syntactic foam decreases the load bearing matrix content, thereby reduces the overall strength of the composites. Further, it is evident that strength of EXXT foams is more in contrast to EXXU for the same filler content. Considering the advantages of weight saving potential and higher modulus offered by EXXT foams, decrease in strength can be considered as very marginal as compared to neat epoxy samples. Fig. 5d presents the specific strength of all the samples. Specific values of pure epoxy specimens are higher as compared to untreated foams but lower as compared to treated foams. Specific compressive strength values of untreated foams decrease by 5–14, 3–9, 1–6% while it increases for treated foams by 2–6, 3–6, 4–6% at 10^{-3}, 10^{-2} and 10^{-1} s^{-1} strain rates respectively as compared to E0. Densification point [65] and associated results are presented in Table 1. The densification stress decreases with decreasing strain rate for all the foams.

Untreated foams have inferior bonding between their constituents. As a result, the peak stress values vary significantly as compared to treated foams for decreasing strain rates. At higher strain rates in such cases, the load taken by the cenosphere particles during compression might get uniformly distributed resulting higher peak stress values. In case of decreasing strain rates, particles deformation is more pronounced leading to lower peak stress values.

3.2.3. Energy absorption

Syntactic foams are extensively used in packaging applications owing to their enhanced ability to energy absorption as compared to neat resin. Such typical characteristic of these foams in energy absorption makes them the best suited as cores in sandwich structures. In stress-strain profile of the samples, it is desired to have an extended stress plateau foams stiffness enhancement. Plastic strain in the matrix increases owing to higher microballoons content that extends the plateau region [38]. In the present study, energy absorption is calculated from the onset of crack initiation in the matrix until the end of plateau region. Energy absorbed by the syntactic foams for varying filler contents including neat epoxy is represented in Table 1. Neat epoxy presents lower energy absorption for all the strain rates. However, the energy absorbed by the foams increases with increase in the filler content for both EXXU and EXXT foams. Further, silane treated syntactic foams show better energy absorption capacity compared to E0 and EXXU foams. Surface modification of cenospheres enhances the bonding between the constituents resulting in matrix stiffening. Increase in cenosphere content further enhances the stiffness of the

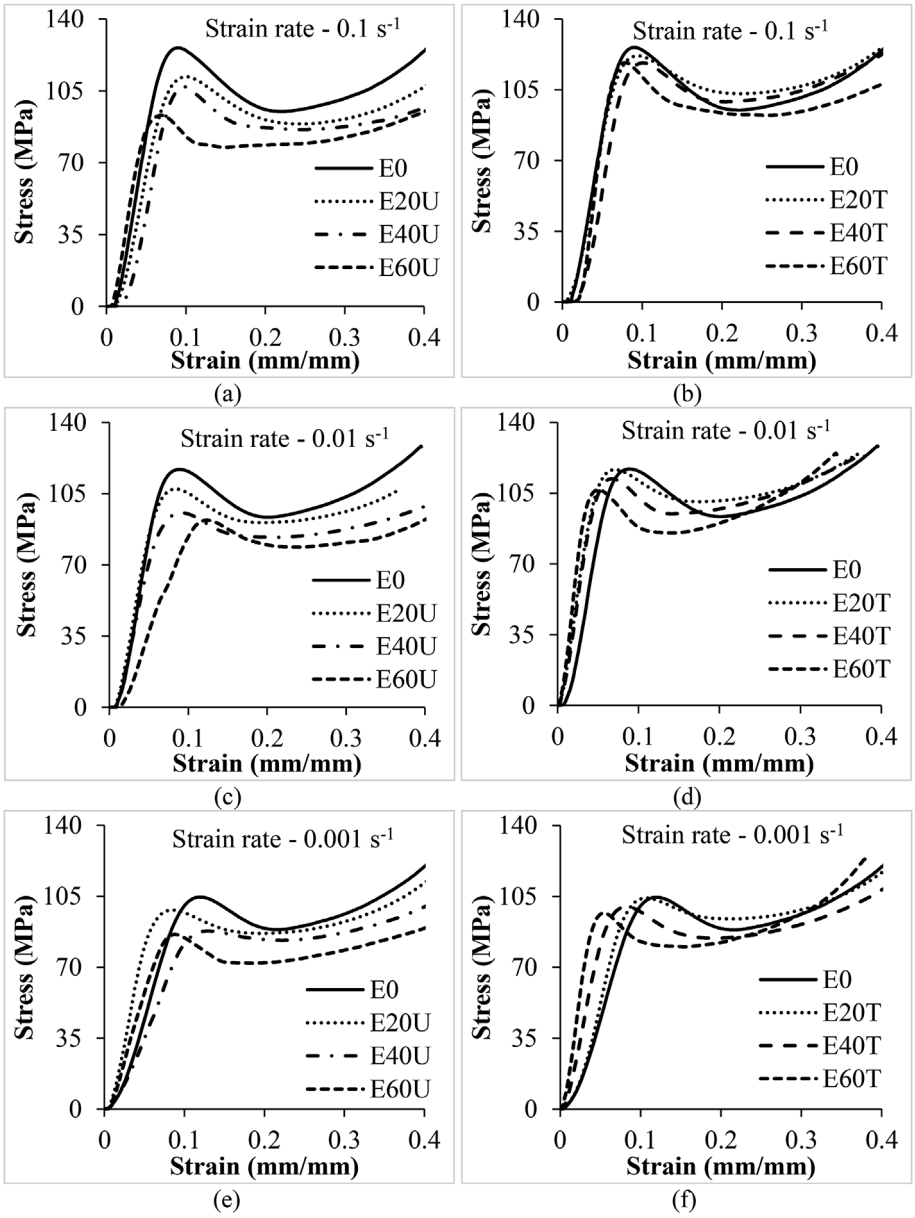

Fig. 3. Representative stress-strain behavior at different strain rates.

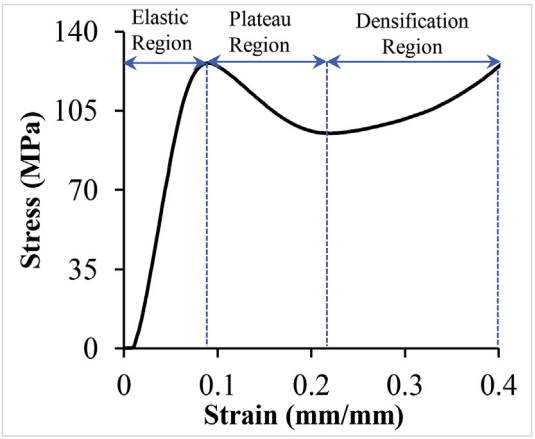

Fig. 4. Representative quasi-static stress-strain behavior of foams.

sample and helps in attaining better energy absorption.

3.2.4. Micrography of post compression samples

Micrographs of neat epoxy and syntactic foams with lower (E20) and higher (E60) filler content for 0.001, 0.01, 0.1 s^{-1} strain rates are depicted by Fig. 6, Fig. 7, Fig. 8 respectively. Even though strain rate changes by two order of magnitude, the differences observed in the failure mechanism of these foams is not sufficient to depict any change as seen from these figures. Extensive deformation of the neat matrix can be seen in Fig. 6a. Similar features are previously observed in the literature [38]. It is seen that few survived cenospheres in EXXU even after densification strain reaches (Fig. 6b). However, EXXT foams owing to silane treatment are noted to absorb more energy during the compression (Fig. 6c). Micrographs for E60U and E60T samples are depicted by Fig. 6d and e respectively. Higher number of intact cenospheres is observed in E60U foams (Fig. 6d). Further, it is revealed that even though there are intact cenospheres, poor bonding between the constituents restricts the foam ability to resist further compression. Micrograph of E60T reveals that strongly bonded and fragmented

Table 1
Compression properties of the samples for different strain rates.

Sample	Strain rate (s^{-1})	Elastic Modulus (GPa)	Yield strength (MPa)	Yield strain (%)	Energy absorption (MJ/mm^3)	Densification stress (MPa)	Densification strain (%)
E0	10^{-1}	1.86 ± 0.037	126.04 ± 2.52	8.92 ± 0.17	38.73 ± 0.77	–	–
	10^{-2}	1.76 ± 0.035	116.93 ± 2.33	9.03 ± 0.18	37.86 ± 0.75	–	–
	10^{-3}	0.96 ± 0.019	104.62 ± 2.09	11.99 ± 0.23	36.33 ± 0.72	–	–
E20U	10^{-1}	2.16 ± 0.043	111.94 ± 2.23	8.37 ± 0.16	41.77 ± 0.83	88.95 ± 1.77	24.52 ± 0.49
	10^{-2}	2.23 ± 0.044	107.30 ± 2.14	8.52 ± 0.17	40.31 ± 0.80	90.74 ± 1.81	19.71 ± 0.39
	10^{-3}	0.97 ± 0.019	98.17 ± 1.96	9.93 ± 0.19	38.43 ± 0.76	86.71 ± 1.73	19.98 ± 0.39
E40U	10^{-1}	2.29 ± 0.045	107.02 ± 2.14	9.12 ± 0.18	42.09 ± 0.84	86.20 ± 1.72	24.98 ± 0.49
	10^{-2}	2.02 ± 0.040	95.64 ± 1.91	9.74 ± 0.19	39.02 ± 0.78	83.52 ± 1.67	20.58 ± 0.41
	10^{-3}	1.31 ± 0.026	87.82 ± 1.75	12.94 ± 0.25	39.01 ± 0.78	83.21 ± 1.66	22.29 ± 0.44
E60U	10^{-1}	2.39 ± 0.047	93.14 ± 1.86	6.96 ± 0.13	45.17 ± 0.90	77.56 ± 1.55	14.95 ± 0.29
	10^{-2}	2.35 ± 0.047	91.95 ± 1.83	8.82 ± 0.17	43.38 ± 0.86	72.60 ± 1.45	11.98 ± 0.23
	10^{-3}	1.99 ± 0.039	86.12 ± 1.72	12.32 ± 0.24	39.15 ± 0.78	71.97 ± 1.43	18.56 ± 0.37
E20T	10^{-1}	2.67 ± 0.053	121.86 ± 2.43	7.07 ± 0.14	39.85 ± 0.79	103.18 ± 2.06	22.58 ± 0.45
	10^{-2}	2.20 ± 0.044	116.65 ± 2.33	9.31 ± 0.18	38.33 ± 0.76	101.04 ± 2.02	19.14 ± 0.38
	10^{-3}	1.73 ± 0.034	104.29 ± 2.08	10.70 ± 0.21	37.89 ± 0.75	93.91 ± 1.87	21.17 ± 0.42
E40T	10^{-1}	2.66 ± 0.053	118.38 ± 2.36	6.76 ± 0.13	39.91 ± 0.79	99.12 ± 1.98	20.56 ± 0.41
	10^{-2}	2.26 ± 0.045	112.12 ± 2.24	8.27 ± 0.16	38.91 ± 0.77	94.80 ± 1.89	14.35 ± 0.28
	10^{-3}	1.99 ± 0.039	99.92 ± 1.99	10.09 ± 0.20	37.79 ± 0.75	84.39 ± 1.68	19.45 ± 0.28
E60T	10^{-1}	3.56 ± 0.071	118.44 ± 2.36	5.04 ± 0.10	46.57 ± 0.93	92.43 ± 1.84	26.02 ± 0.52
	10^{-2}	3.11 ± 0.062	106.64 ± 2.13	5.51 ± 0.11	41.00 ± 0.82	85.33 ± 1.70	14.35 ± 0.28
	10^{-3}	2.91 ± 0.058	96.78 ± 1.93	7.91 ± 0.15	40.47 ± 0.80	80.18 ± 1.60	15.66 ± 0.31

cenospheres are seen to be intact with the matrix (Fig. 6e). Compressive loading appears to fragment the silane treated cenospheres easily as compared to EXXU due to more brittleness resulting from surface modifies fillers. However, strong bonding between the constituents tends to offer more resistance to compression, post cenospheres fragmentation. It is clearly evident from Fig. 6e that the strongly bonded cenospheres have been compressed to the maximum extent before and after the fragmentation of cenospheres. Such events enhance the overall

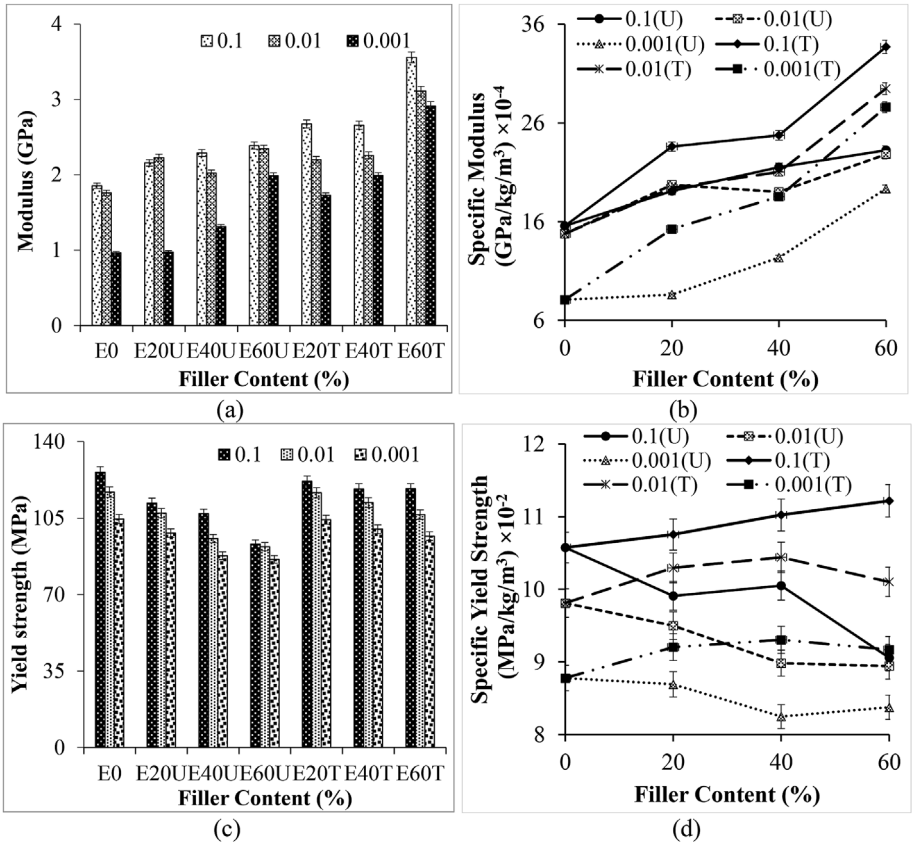

Fig. 5. Experimentally measured quasi-static compression (a) modulus (b) specific modulus (c) yield strength and (d) specific yield strength of the samples.

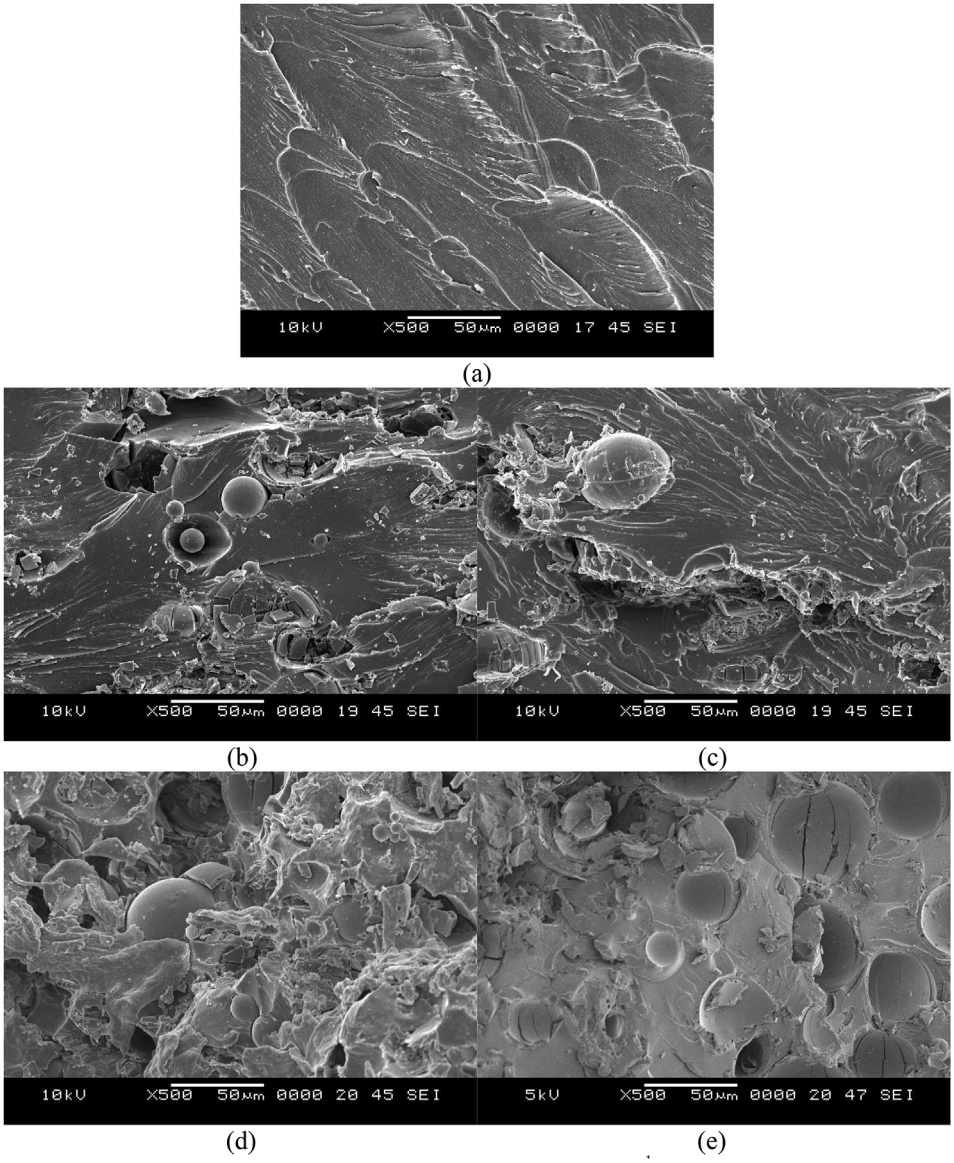

Fig. 6. Post compression micrographs of samples at 0.001 s^{-1} (a) E0 (b) E20U (c) E20T (d) E60U and (e) E60T.

resistance to compressive loading.

3.2.5. Property map

Property map is presented Fig. 9 that might act as a guideline for industrial practitioners in choosing suitable composition as demanded by the application. Compressive modulus at a strain rate of 10^{-3} s^{-1} are plotted as a function of density for composites having different reinforcements in Fig. 9 [38,39]. Extracted data from the available literature is compared with the experimental data (Fig. 9). It is observed that the composites with lower density exhibit lower compressive modulus. However, the advantage of naturally available and cost effective hollow fly ash cenospheres filled lightweight syntactic foams is clearly evident in Fig. 9. Density of all the foams including pure epoxy is higher compared to other composites investigated in the literature. Hollow glass microballoons and ceramic microballoons are engineered. Thereby, the density associated with these foams is lower as compared fly ash cenospheres. However, fly ash cenospheres are naturally available, thereby control over the density is difficult. Syntactic foams tested in the present study outperform hollow glass microballoon/epoxy and ceramic microballoon/epoxy composites. Compressive modulus is significantly higher for higher filler contents of cenospheres (E60). E60T foam reveals the highest modulus as compared to all other composites. Therefore, from the property map it can be concluded that cenosphere/epoxy syntactic foams with higher cenosphere contents provide higher modulus as compared to other composites signifying their aptness in weight sensitive applications. Abundant availability of environment pollutant fly ash cenospheres can be effectively utilized to prepare foams for various applications based on such specific requirements.

3.3. Dynamic mechanical analysis

DMA is the materials ability to convert mechanical energy into heat energy under external load (*Tan δ*). As a general characteristic, the plots have three distinct regions as presented in Fig. 10. Region I depicts decrease in storage modulus with temperature rise. In region II, storage modulus reduces significantly with increase in temperature. This is attributed to the sample reaching its glass transition temperature. In region III, storage modulus stabilizes to a very low value compared to that in region I. Flow region is defined by Region III wherein variation of storage modulus is negligible.

Storage modulus at 30, 60, 90 and 175 °C (Fig. 10), are presented in Table 2 to determine the extent of variation of storage modulus with

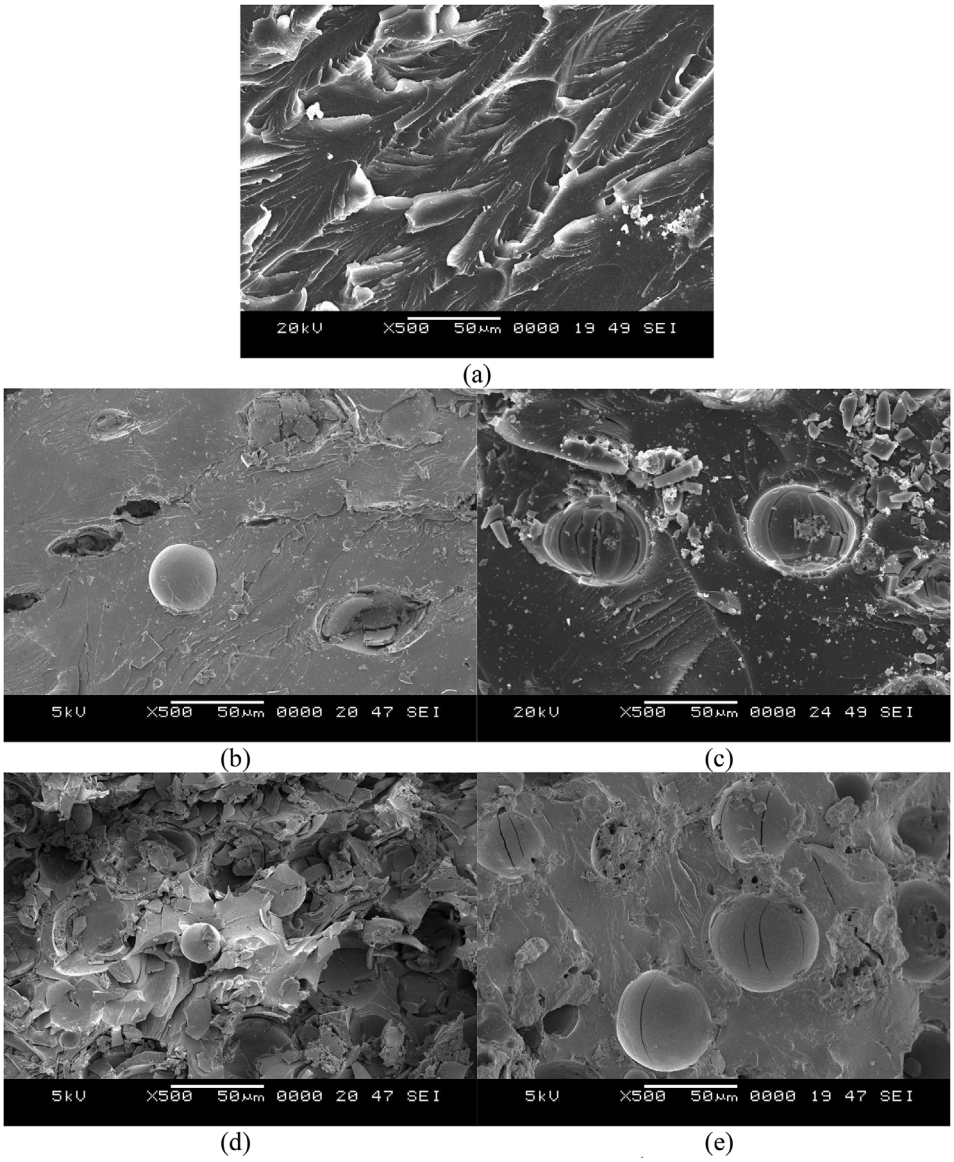

Fig. 7. Post compression micrographs of samples at 0.01 s^{-1} (a) E0 (b) E20U (c) E20T (d) E60U and (e) E60T.

respect to temperature. Selection of these representative temperatures is based on the observations that,

- 28 °C is defined as the room temperature for this study and is important for a large number of applications.
- In region I, trend of storage modulus is linear and the graphs are well separated in the temperature range of 28–60 °C, enabling selection of representative temperature of 60 °C to demonstrate the dependence of storage modulus on cenosphere content.
- In region II around 90 °C, the storage modulus decreases drastically after attaining glass transition temperature.
- In region III, 175 °C is maximum temperature of the test. It is observed that no variation in storage modulus with respect to temperature is observed. Thereby, any temperature value can be selected for illustration of the trends.

3.3.1. Storage modulus

Fig. 11 presents the temperature dependence of storage modulus of all specimens measured at 1 Hz. With temperature rise, storage modulus decreases steadily within the temperature range of 28–60 °C and drops sharply thereafter. Storage modulus for neat epoxy is lower than the foams in region I. E60T syntactic foams presents highest storage modulus (Fig. 11). Increase in cenosphere volume fraction results in higher storage modulus [66]. This is accredited to lower molecular movement of epoxy molecules due to cenosphere addition. However, silane treated foams present higher storage modulus as compared to untreated ones owing to superior adhesion between the constituents resulting in higher foam stiffness [67]. Storage modulus increases in the range of 13–43% and 28–57% for EXXU and EXXT foams, respectively as compared to E0.

In region II, all the samples reach glass transition temperature, as a result, storage modulus decreases drastically due to change from glassy to rubbery state. Region III is characterized by lowest storage modulus for the neat resin and is measured to be in the range of 105–325% and 258–370% lower than untreated and treated syntactic foams respectively (Fig. 11). In this region, storage modulus increases with cenosphere volume fraction but does not show significant change with respect to silane treatment of cenospheres. However, the retention of properties at elevated temperatures in EXXT foams can be beneficial for wide range of applications.

Maximum utility temperature (T_{max}) of samples is defined as the temperature for which storage modulus starts to decrease drastically

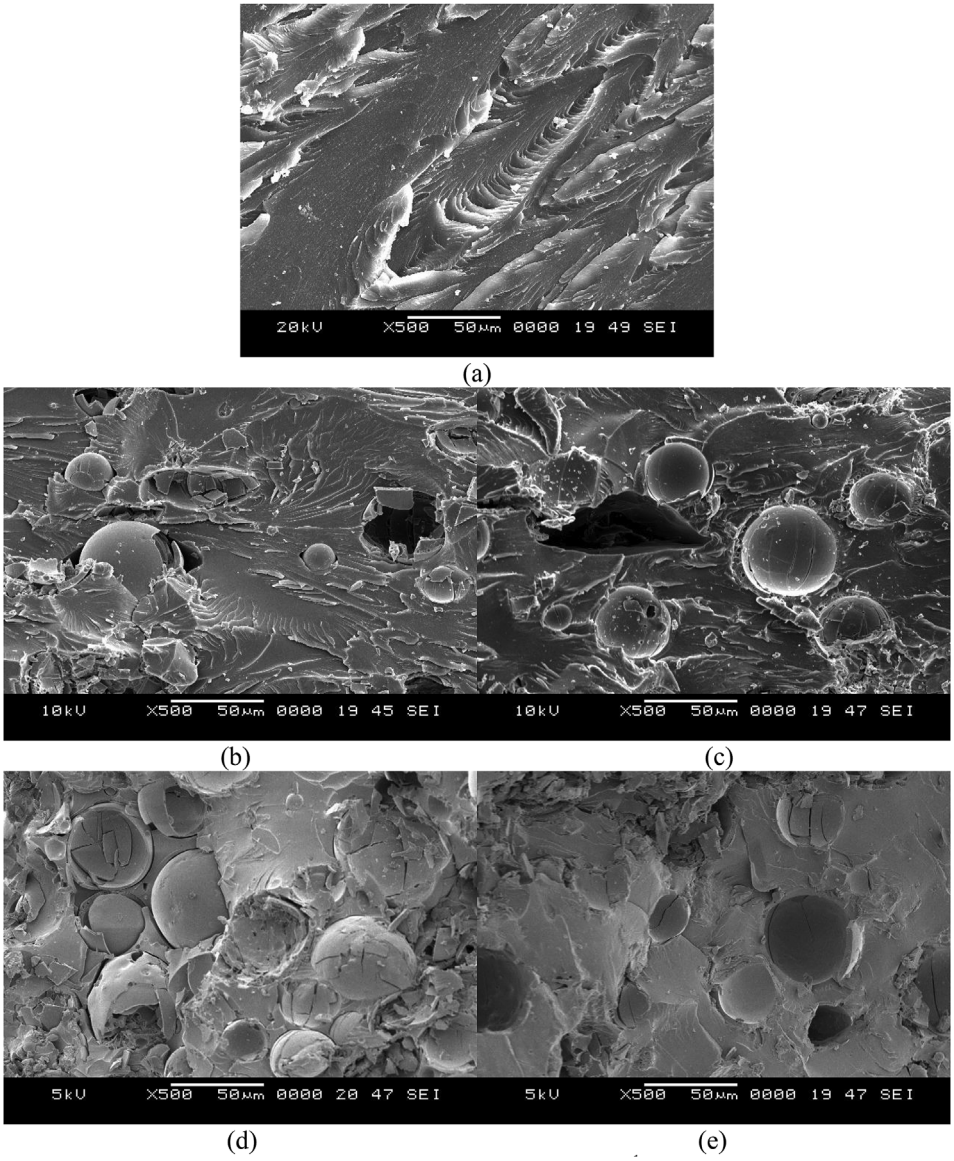

Fig. 8. Post compressive micrography of samples at 0.1 s^{-1} (a) E0 (b) E20U (c) E20T (d) E60U and (e) E60T.

[47,68]. Intersection point of the tangents drawn to the curve in regions I and II in Fig. 10 is defined as T_{max}. The values of T_{max} and glass transition temperature are presented in Table 3. T_{max} is lower for E0 as compared to foams. Compared to the T_{max} of neat epoxy (61 °C), syntactic foams have T_{max} above 65 °C. However, increase in T_{max} is observed for syntactic foams with increasing filler content.

3.3.2. Loss modulus

Fig. 12 shows the sets of graphs for loss modulus variation with temperature for all the samples. Loss modulus reaches peak around 61 °C and decreases thereafter. It might be due to non-crystalline phase presence in matrix. T_g of the matrix is found to be around 76 °C. Further, the values of loss modulus diminish to zero as temperature surges over 90 °C. T_g is defined as the corresponding temperature to the maximum loss modulus curve and is available in Ref's [47,69]. T_g of E0 is higher than all foam samples. T_g of foams decreases with cenosphere loading. Maximum loss modulus values are presented in Table 4. Some of the notable trends in the loss modulus behavior are:

- In region I, loss modulus is lower for foams as compared to the neat resin except for treated sample with 60 vol.% of cenospheres owing to the lower internal sliding of epoxy molecules and sliding between the cenospheres and matrix interface. Lower filler content makes matrix viscoelasticity to contribute more as compared to frictional energy dissipation. At higher filler content, reduction in the influence of matrix viscoelasticity is observed owing to extreme dilution effect of the cenospheres into the matrix. Thereby, the internal molecules movement within the matrix becomes difficult, hindering the chain segments energy dissipation leading to lower heating losses [67].
- Increase in temperature post 60 °C and higher filler content increases the peak intensity.

3.3.3. Damping

Damping capability (Tan δ) the material is computed using the ratio of loss and storage modulus [70] and is given by,

$$Tan\ \delta = \frac{E''}{E'} \quad (1)$$

Tan δ is an important parameter to characterize the viscoelastic behavior. Fig. 13 shows the representative sets of plots for variation of *Tan δ* with respect to temperature for all the samples. Increase in volume

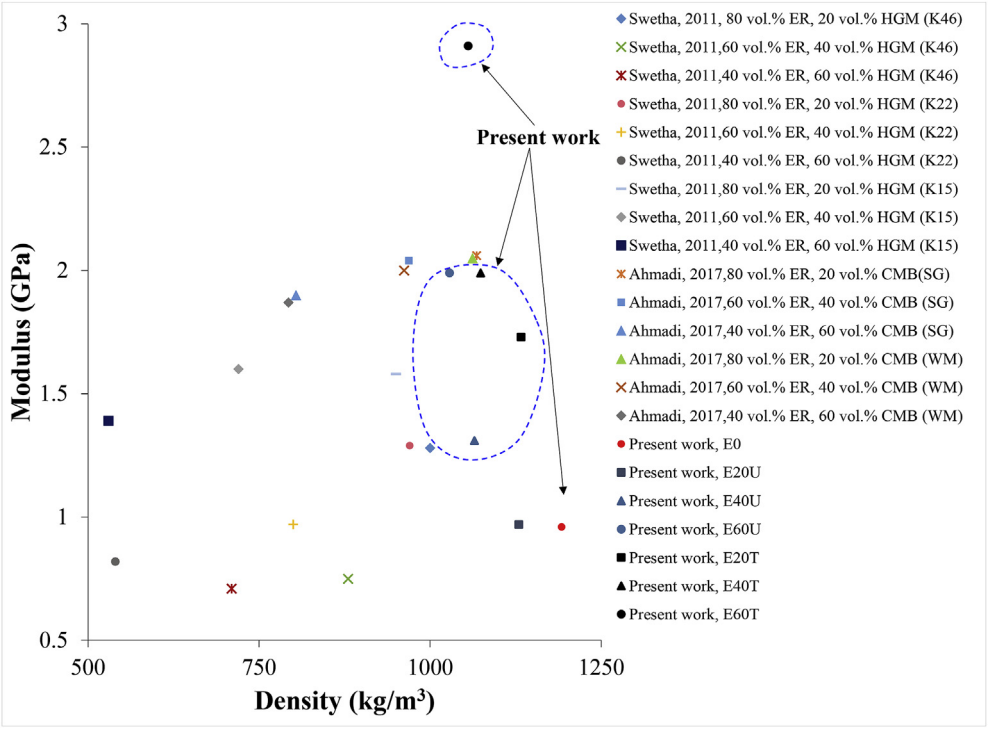

Fig. 9. Compressive modulus plotted against density from available studies [38,39]. Note: ER – Epoxy resin, HGM – Hollow glass microballoons, CMB – Ceramic microballoons.

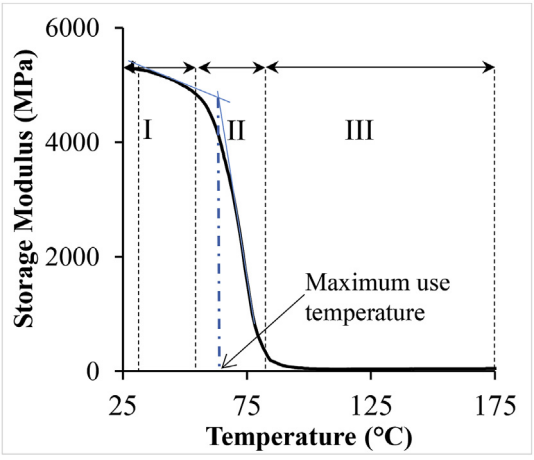

Fig. 10. Schematic representation of variation of storage modulus against temperature for the samples. Regions I, II, and III are identified by arrows. The dashed lines correspond to 30, 60, 90 and 175 °C where storage modulus values are noted and presented in Table 2.

fraction results in increasing *Tan δ* (Fig. 13). Neat resin and foam samples exhibit maximum *Tan δ* at approximately the same value implying matrix properties determine damping. Increase in cenosphere volume fraction reduces area under *Tan δ* curve (Fig. 13). Increase in stability of the polymer materials is attributed with decrease in *Tan δ* area plot [42]. This implies that with increasing filler content, stability of foams at higher temperatures increases. Foam properties are significantly affected by the operating temperature, volume fraction and surface modification of cenospheres. Initially *Tan δ* increases and later noted to be decreasing with increasing temperature. Neat epoxy reveals lower *Tan δ* values as compared to all the syntactic foams, demonstrating damping enhancement with cenosphere addition. However, EXXT foams reveal higher values of *Tan δ* for all filler volume fractions. Peak *Tan δ* value of 0.914 is noted at 87 °C for E60T foam which is higher as compared to all other foams and neat epoxy. Furthermore, comparing the *Tan δ* value of the matrix with the syntactic foams, it is observed that the filler addition improves the damping capability. This is attributed to contributions of in-built porous structure (hollow space) in cenospheres and frictional damping. Increase in filler content further leads to incremental energy loss leading to increasing damping loss factor [71,72]. Surface treatment of cenospheres enhances the bonding

Table 2
Comparison of storage modulus at four representative temperatures.

Material	Storage Modulus (MPa)			
	30 °C	60 °C	90 °C	175 °C
E0	5275.62 ± 105.51	4507.34 ± 90.14	90.30 ± 1.80	45.30 ± 0.90
E20U	5983.13 ± 119.66	5513.82 ± 110.27	110.30 ± 2.20	92.77 ± 1.85
E40U	6908.12 ± 138.16	6316.76 ± 126.33	195.99 ± 3.91	109.79 ± 2.19
E60U	7526.96 ± 150.53	6962.18 ± 139.24	309.52 ± 6.19	192.32 ± 3.84
E20T	6759.16 ± 135.18	6311.65 ± 126.23	222.75 ± 4.45	162.36 ± 3.24
E40T	7248.21 ± 144.96	6711.07 ± 134.22	251.41 ± 5.02	193.21 ± 3.86
E60T	8275.87 ± 165.51	7426.27 ± 148.52	293.94 ± 5.87	212.89 ± 4.25

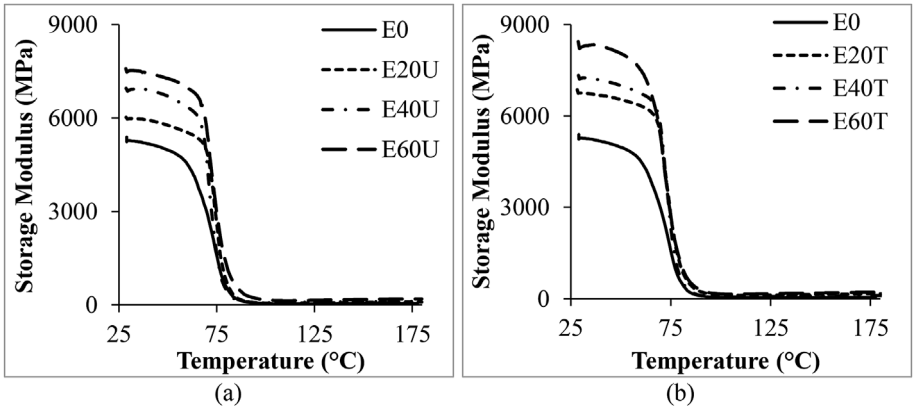

Fig. 11. Experimentally measured storage modulus.

Table 3
Maximum sample utility and T_g for all specimens.

Material	Maximum sample utility temperature T_{max} (°C)	Glass transition temperature T_g (°C)
E0	61.54 ± 1.23	76.22 ± 1.52
E20U	67.20 ± 1.34	75.95 ± 1.51
E40U	69.05 ± 1.38	74.82 ± 1.49
E60U	71.24 ± 1.42	74.15 ± 1.48
E20T	66.32 ± 1.32	75.40 ± 1.50
E40T	68.52 ± 1.37	74.33 ± 1.48
E60T	69.74 ± 1.39	74.00 ± 1.48

Table 4
Maximum and room temperature loss modulus values of all the samples.

Material	Loss modulus at 30 °C (MPa)	Maximum loss modulus (MPa)
E0	327.17 ± 6.54	628.64 ± 12.57
E20U	229.23 ± 4.58	798.48 ± 15.96
E40U	298.91 ± 5.97	917.40 ± 18.34
E60U	316.43 ± 6.32	999.25 ± 19.98
E20T	244.61 ± 4.89	925.68 ± 18.51
E40T	302.56 ± 6.05	978.14 ± 19.56
E60T	338.51 ± 6.77	1060.46 ± 21.20

of the constituents enhancing stability further.

3.3.4. Morphology of DMA samples

Freeze fracture features of all the samples post DMA is shown in Fig. 14. Micrographs are captured post temperature sweep on the samples. Deformation marks are observed on the surface of neat epoxy indicating plastic deformation (Fig. 14a). At elevated temperature, neat epoxy undergoes more deformation owing to more induced viscoelasticity. As a result, neat samples undergo more plastic deformation. Such an observation is not observed for E20 samples (Fig. 14b and c). Reinforcing hard shelled cenospheres into the matrix reduces deformation of the foams considerably. Cenospheres absorb the deformation transferred from the matrix effectively. Increasing the cenosphere content in the system reduces the matrix deformation further (Fig. 14d and e). As a result, material tends to absorb more energy at elevated temperatures resulting in enhanced stiffness as compared to foams with lower cenosphere content and neat epoxy samples. Treated syntactic foams exhibited higher stiffness and damping as compared to untreated syntactic foams and neat epoxy owing to better bonding between the constituents.

4. Conclusions

In the present work, quasi-static compression response and temperature effect on the dynamic mechanical behavior of syntactic foams is presented. Combination of cenosphere volume fraction and surface treatment are analyzed. Quasi-static compressive response for varying filler contents of untreated and treated syntactic foams reveals that,

- Neat epoxy sample has the lowest modulus among all the samples. Increase in the cenosphere volume fraction increases the modulus of elasticity in the range of 0–48% for EXXU and 3–44% for EXXT foams respectively.
- Increase in cenosphere volume fraction decreases the strength of EXXU and EXXT foams in the range of 11–28 and 3–8% respectively

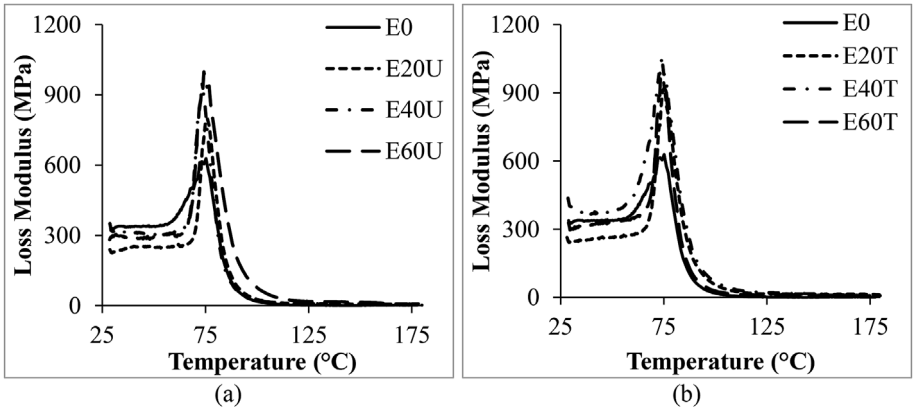

Fig. 12. Experimentally measured loss modulus.

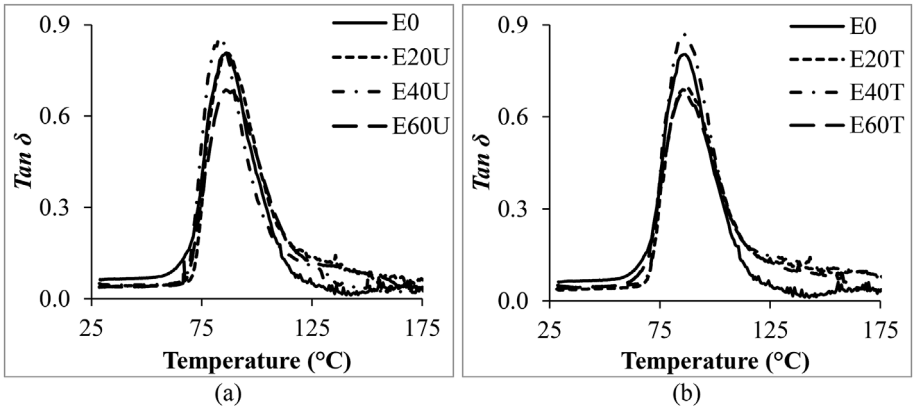

Fig. 13. Experimentally measured tan δ of all samples.

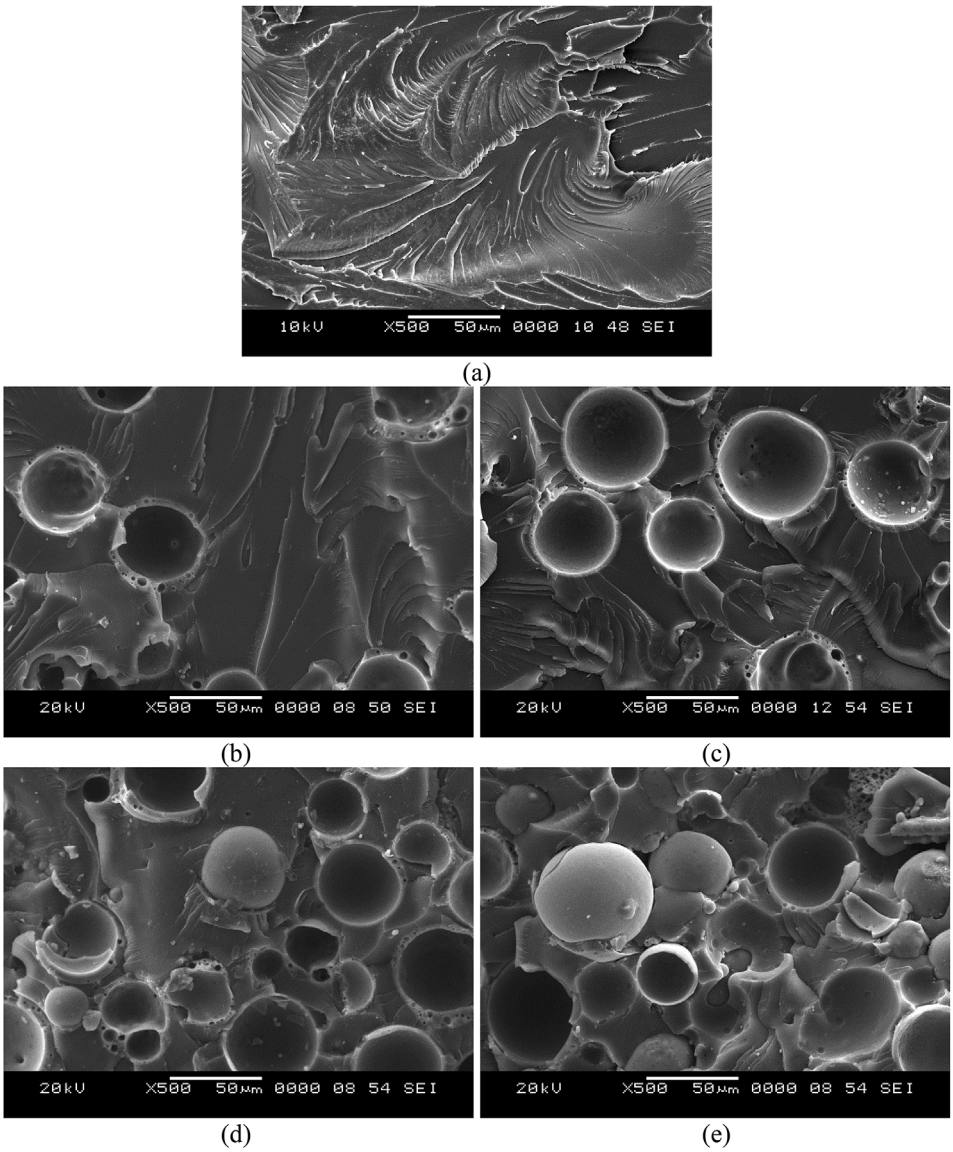

Fig. 14. Micrographs of (a) Neat epoxy (b) E20U (c) E20T (d) E60U and (e) E60T post DMA tests.

against E0.

- Energy absorption of the foam increases with increasing cenosphere loading for all the foam samples.
- E60T sample presents the highest energy absorption among all the samples.

DMA of the syntactic foams reveal,

- Neat epoxy sample presents lowest storage modulus as compared to EXXT. Increase in cenosphere volume fraction results in increase of storage modulus for both EXXU and EXXT foams.
- Storage modulus of neat resin is lower by 105–325 and 258–370% as compared to EXXU and EXXT respectively.
- Loss modulus of syntactic foams is lower than E0 owing to constrained epoxy resin movement in the vicinity of cenosphere particles.
- Presence of cenospheres helps in increasing the retention of mechanical properties of syntactic foams at temperatures beyond T_g.
- Addition of fly ash cenospheres enhances the damping capacity of the foams. Peak *Tan δ* value of 0.914 appears at 87 °C for E60-T foam which is higher as compared to all other foams and neat epoxy.

References

[1] Shutov F. Syntactic polymer foams. Chromatography/foams/copolymers. 1986. p. 63–123.
[2] Gupta N, Zeltmann SE, Shunmugasamy VC, Pinisetty D. Applications of polymer matrix syntactic foams. JOM 2014;66(2):245–54.
[3] Grosjean F, Bouchonneau N, Choqueuse D, Sauvant-Moynot V. Comprehensive analyses of syntactic foam behaviour in deepwater environment. J Mater Sci 2009;44(6):1462–8.
[4] Hobaica EC, Cook SD. The characteristics of syntactic foams used for buoyancy. J Cell Plast 1968;4(4):143–8.
[5] Gupta N, Kishore E Woldesenbet, Sankaran S. Studies on compressive failure features in syntactic foam material. J Mater Sci 2001;36(18):4485–91.
[6] Gupta N, Woldesenbet E, hore K, Sankaran S. Response of syntactic foam core sandwich structured composites to three-point bending. J Sandw Struct Mater 2002;4(3):249–72.
[7] Licitra L, Luong DD, Strbik OM, Gupta N. Dynamic properties of alumina hollow particle filled aluminum alloy A356 matrix syntactic foams. Mater Des 2015;66:504–15.
[8] Labella M, Shunmugasamy VC, Strbik OM, Gupta N. Compressive and thermal characterization of syntactic foams containing hollow silicon carbide particles with porous shell. J Appl Polym Sci 2014;131(17).
[9] Xie W, Yan H, Mei Q, Du M, Huang Z. Compressive and fracture properties of syntactic foam filled with hollow plastic bead(HPC). J Wuhan Univ Technol -Materials Sci Ed 2007;22(3):499–501.
[10] Yusriah L, Mariatti M. Effect of hybrid phenolic hollow microsphere and silica-filled vinyl ester composites. J Compos Mater 2013;47(2):169–82.
[11] Wang L, Yang X, Zhang J, Zhang C, He L. The compressive properties of expandable microspheres/epoxy foams. Compos B Eng 2014;56:724–32.
[12] Yung KC, Zhu BL, Yue TM, Xie CS. Preparation and properties of hollow glass microsphere-filled epoxy-matrix composites. Compos Sci Technol 2009;69(2):260–4.
[13] Mohan VB, Lau K-t, Hui D, Bhattacharyya D. Graphene-based materials and their composites: a review on production, applications and product limitations. Compos B Eng 2018;142:200–20.
[14] Lau K-t, Hung P-y, Zhu M-H, Hui D. Properties of natural fibre composites for structural engineering applications. Compos B Eng 2018;136:222–33.
[15] Chhetri S, Adak NC, Samanta P, Murmu NC, Hui D, Kuila T, Lee JH. Investigation of the mechanical and thermal properties of l-glutathione modified graphene/epoxy composites. Compos B Eng 2018;143:105–12.
[16] Zhang Y, Rhee KY, Hui D, Park S-J. A critical review of nanodiamond based nanocomposites: synthesis, properties and applications. Compos B Eng 2018;143:19–27.
[17] Hung P-y, Lau K-t, Cheng L-k, Leng J, Hui D. Impact response of hybrid carbon/glass fibre reinforced polymer composites designed for engineering applications. Compos B Eng 2018;133:86–90.
[18] Safri SNA, Sultan MTH, Jawaid M, Jayakrishna K. Impact behaviour of hybrid composites for structural applications: a review. Compos B Eng 2018;133:112–21.
[19] Mathapati M, Ramesh MR, Doddamani M. High temperature erosion behavior of plasma sprayed NiCrAlY/WC-Co/cenosphere coating. Surf Coating Technol 2017;325:98–106.
[20] Manakari Vyasaraj, Parande Gururaj, Doddamani Mrityunjay, Gupta M. Enhancing the ignition, hardness and compressive response of magnesium by reinforcing with hollow glass microballoons. Materials 2017;10(9):15.
[21] Singh AK, Patil B, Hoffmann N, Saltonstall B, Doddamani M, Gupta N. Additive manufacturing of syntactic foams: Part 1: development, properties, and recycling potential of filaments. JOM 2018;70(3):303–9.
[22] Singh AK, Saltonstall B, Patil B, Hoffmann N, Doddamani M, Gupta N. Additive manufacturing of syntactic foams: Part 2: specimen printing and mechanical property characterization. JOM 2018;70(3):310–4.
[23] Gupta N, Singh Brar B, Woldesenbet E. Effect of filler addition on the compressive and impact properties of glass fibre reinforced epoxy. Bull Mater Sci 2001;24(2):219–23.
[24] Rohatgi PK, Weiss D, Gupta N. Applications of fly ash in synthesizing low-cost MMCs for automotive and other applications. JOM 2006;58(11):71–6.
[25] Li J, Agarwal A, Iveson SM, Kiani A, Dickinson J, Zhou J, Galvin KP. Recovery and concentration of buoyant cenospheres using an Inverted Reflux Classifier. Fuel Process Technol 2014;123:127–39.
[26] Blissett RS, Rowson NA. A review of the multi-component utilisation of coal fly ash. Fuel 2012;97:1–23.
[27] Anshits NN, Mikhailova OA, Salanov AN, Anshits AG. Chemical composition and structure of the shell of fly ash non-perforated cenospheres produced from the combustion of the Kuznetsk coal (Russia). Fuel 2010;89(8):1849–62.
[28] Mondal DP, Das S, Jha N. Dry sliding wear behaviour of aluminum syntactic foam. Mater Des 2009;30(7):2563–8.
[29] B.K.B R, Eric ZS, Mrityunjay D, Nikhil G, Uzma GS, S.R.R N. Effect of cenosphere surface treatment and blending method on the tensile properties of thermoplastic matrix syntactic foams. J Appl Polym Sci 2016;133(35).
[30] Kumar BRB, Doddamani M, Zeltmann SE, Gupta N, Ramakrishna S. Data characterizing tensile behavior of cenosphere/HDPE syntactic foam. Data in Brief 2016;6:933–41.
[31] Zeltmann SE, Bharath Kumar BR, Doddamani M, Gupta N. Prediction of strain rate sensitivity of high density polyethylene using integral transform of dynamic mechanical analysis data. Polymer 2016;101:1–6.
[32] Shahapurkar K, Garcia CD, Doddamani M, Mohan Kumar GC, Prabhakar P. Compressive behavior of cenosphere/epoxy syntactic foams in arctic conditions. Compos B Eng 2018;135:253–62.
[33] Waddar, S., P. Jeyaraj, and M. Doddamani, Influence of axial compressive loads on buckling and free vibration response of surface-modified fly ash cenosphere/epoxy syntactic foams. J Compos Mater. 0(0): p. 0021998317751284.
[34] Garcia CD, Shahapurkar K, Doddamani M, Kumar GCM, Prabhakar P. Effect of arctic environment on flexural behavior of fly ash cenosphere reinforced epoxy syntactic foams. Compos B Eng 2018;151:265–73.
[35] Qiao J, Wu G. Tensile properties of fly ash/polyurea composites. J Mater Sci 2011;46(11):3935–41.
[36] Manakari V, Parande G, Doddamani M, Gaitonde VN, Siddhalingeshwar IG, Kishore, Shunmugasamy VC, Gupta N. Dry sliding wear of epoxy/cenosphere syntactic foams. Tribol Int 2015;92(Supplement C):425–38.
[37] Kumar Bharath, R B, Singh AK, Doddamani M, Luong DD, Gupta N. Quasi-static and high strain rate compressive response of injection-molded cenosphere/HDPE syntactic foam. JOM 2016;68(7):1861–71.
[38] Swetha C, Kumar R. Quasi-static uni-axial compression behaviour of hollow glass microspheres/epoxy based syntactic foams. Mater Des 2011;32(8):4152–63.
[39] Ahmadi H, Liaghat G, Shokrieh M, Hadavinia H, Ordys A, Aboutorabi A. Quasi-static and dynamic compressive properties of ceramic microballoon filled syntactic foam. J Compos Mater 2015;49(10):1255–66.
[40] Jayavardhan ML, Doddamani M. Quasi-static compressive response of compression molded glass microballoon/HDPE syntactic foam. Compos B Eng 2018;149:165–77.
[41] Zeltmann SE, G N, Bharat Kumar BR, Doddamani Mrityunjay. Dynamic mechanical analysis of cenosphere/hdpe syntactic foams. Proceedings of the American society for composites. Williamsburg, United States: DEStech Publications Inc; 2016.
[42] Shunmugasamy VC, Pinisetty D, Gupta N. Viscoelastic properties of hollow glass particle filled vinyl ester matrix syntactic foams: effect of temperature and loading frequency. J Mater Sci 2013;48(4):1685–701.
[43] Das A, Satapathy BK. Structural, thermal, mechanical and dynamic mechanical properties of cenosphere filled polypropylene composites. Mater Des 2011;32(3):1477–84.
[44] Tagliavia G, Porfiri M, Gupta N. Vinyl ester—glass hollow particle composites: dynamic mechanical properties at high inclusion volume fraction. J Compos Mater 2009;43(5):561–82.
[45] Lin TC, Gupta N, Talalayev A. Thermoanalytical characterization of epoxy matrix-glass microballoon syntactic foams. J Mater Sci 2009;44(6):1520–7.
[46] Jian G, Gaohui W, Xiao Z. Effect of surface-modification on the dynamic behaviors of fly ash cenospheres filled epoxy composites. Polym Compos 2009;30(2):232–8.
[47] Sankaran S, Sekhar KR, Raju G, Kumar MNJ. Characterization of epoxy syntactic foams by dynamic mechanical analysis. J Mater Sci 2006;41(13):4041–6.
[48] Zhang X, Wang S, Xu L, Feng L, Ji Y, Tao L, Li S, Wei Y. Biocompatible polydopamine fluorescent organic nanoparticles: facile preparation and cell imaging. Nanoscale 2012;4(18):5581–4.
[49] Liu M, Zeng G, Wang K, Wan Q, Tao L, Zhang X, Wei Y. Recent developments in polydopamine: an emerging soft matter for surface modification and biomedical applications. Nanoscale 2016;8(38):16819–40.
[50] Zhang X, Huang Q, Liu M, Tian J, Zeng G, Li Z, Wang K, Zhang Q, Wan Q, Deng F, Wei Y. Preparation of amine functionalized carbon nanotubes via a bioinspired strategy and their application in Cu2+ removal. Appl Surf Sci 2015;343:19–27.
[51] Liu M, Ji J, Zhang X, Zhang X, Yang B, Deng F, Li Z, Wang K, Yang Y, Wei Y. Self-polymerization of dopamine and polyethyleneimine: novel fluorescent organic nanoprobes for biological imaging applications. J Mater Chem B 2015;3(17):3476–82.
[52] Shi Y, Liu M, Deng F, Zeng G, Wan Q, Zhang X, Wei Y. Recent progress and development on polymeric nanomaterials for photothermal therapy: a brief overview. J Mater Chem B 2017;5(2):194–206.
[53] Shi Y, Jiang R, Liu M, Fu L, Zeng G, Wan Q, Mao L, Deng F, Zhang X, Wei Y. Facile synthesis of polymeric fluorescent organic nanoparticles based on the self-

polymerization of dopamine for biological imaging. Mater Sci Eng C 2017;77:972–7.
[54] Huang L, Liu M, Huang H, Wen Y, Zhang X, Wei Y. Recent advances and progress on melanin-like materials and their biomedical applications. Biomacromolecules 2018;19(6):1858–68.
[55] Huang Q, Liu M, Chen J, Wan Q, Tian J, Huang L, Jiang R, Wen Y, Zhang X, Wei Y. Facile preparation of MoS2 based polymer composites via mussel inspired chemistry and their high efficiency for removal of organic dyes. Appl Surf Sci 2017;419:35–44.
[56] Huang Q, Liu M, Mao L, Xu D, Zeng G, Huang H, Jiang R, Deng F, Zhang X, Wei Y. Surface functionalized SiO2 nanoparticles with cationic polymers via the combination of mussel inspired chemistry and surface initiated atom transfer radical polymerization: characterization and enhanced removal of organic dye. J Colloid Interface Sci 2017;499:170–9.
[57] Zhang X, Huang Q, Deng F, Huang H, Wan Q, Liu M, Wei Y. Mussel-inspired fabrication of functional materials and their environmental applications: progress and prospects. Applied Materials Today 2017;7:222–38.
[58] Kumar Bharath, R B, Doddamani M, Zeltmann SE, Gupta N, Uzma, Gurupadu S, Sailaja RRN. Effect of particle surface treatment and blending method on flexural properties of injection-molded cenosphere/HDPE syntactic foams. J Mater Sci 2016;51(8):3793–805.
[59] Shahapurkar K, Garcia CD, Doddamani M, Mohan Kumar GC, Prabhakar P. Compressive behavior of cenosphere/epoxy syntactic foams in arctic conditions. Compos B Eng 2018;135(Supplement C):253–62.
[60] Gupta N, Priya S, Islam R, Ricci W. Characterization of mechanical and electrical properties of epoxy-glass microballoon syntactic composites. Ferroelectrics 2006;345(1):1–12.
[61] Gupta N, Ye R, Porfiri M. Comparison of tensile and compressive characteristics of vinyl ester/glass microballoon syntactic foams. Compos B Eng 2010;41(3):236–45.
[62] Wouterson EM, Boey FYC, Hu X, Wong S-C. Specific properties and fracture toughness of syntactic foam: effect of foam microstructures. Compos Sci Technol 2005;65(11):1840–50.
[63] Zhang L, Roy S, Chen Y, Chua EK, See KY, Hu X, Liu M. Mussel-inspired polydopamine coated hollow carbon microspheres, a novel versatile filler for fabrication of high performance syntactic foams. ACS Appl Mater Interfaces 2014;6(21):18644–52.
[64] Kim JI, Ryu SH, Chang YW. Mechanical and dynamic mechanical properties of waste rubber powder/HDPE composite. J Appl Polym Sci 2000;77(12):2595–602.
[65] Smith B, Szyniszewski S, Hajjar J, Schafer B, Arwade S. Characterization of steel foams for structural components. Metals 2012;2(4):399.
[66] Gu J, Wu G, Zhang Q. Preparation and damping properties of fly ash filled epoxy composites. Mater Sci Eng, A 2007;452–453:614–8.
[67] Gu J, Wu G, Zhang Q. Effect of porosity on the damping properties of modified epoxy composites filled with fly ash. Scripta Mater 2007;57(6):529–32.
[68] Capela C, Ferreira JAM, Costa JDM. Viscoelastic properties assessment of syntactic foams by dynamic mechanical analysis. Mater Sci Forum 2010;636–637:280–6.
[69] Ray D, Sarkar BK, Das S, Rana AK. Dynamic mechanical and thermal analysis of vinylester-resin-matrix composites reinforced with untreated and alkali-treated jute fibres. Compos Sci Technol 2002;62(7):911–7.
[70] Zhu J, Wei S, Ryu J, Budhathoki M, Liang G, Guo Z. In situ stabilized carbon nanofiber (CNF) reinforced epoxy nanocomposites. J Mater Chem 2010;20(23):4937–48.
[71] Gupta N, Woldesenbet E. Microballoon wall thickness effects on properties of syntactic foams. J Cell Plast 2004;40(6):461–80.
[72] Shunmugasamy VC, Pinisetty D, Gupta N. Thermal expansion behavior of hollow glass particle/vinyl ester composites. J Mater Sci 2012;47(14):5596–604.